Jurnal Krisnadana (Jurnal Komputer, Sistem Kendali & Jaringan)
Vol 5, Issue 3, May 2026, pp. 700-712
https://doi.org/10.58982/tegv3p18

E-ISSN: 2808-3563
P-ISSN: 2808-3520

Tuna Eye Image Classification for Freshness Detection Using PCA and SVM

I Made Dwi Putra Asana[1*], I Wayan Aldinata[2], Ni Putu Suci Meinarni[3], Made Leo Radhitya[4], Ida Bagus Gede Anandita[5]

[1*,2,3,4,5] *Department of Informatics, Institut Bisnis dan Teknologi Indonesia, Denpasar, Indonesia*
[1*]*dwiputraasana@instiki.ac.id*; [2]*aldinata@gmail.com*; [3]*sucimeinarni@instiki.ac.id*; [4]*leo.radhitya@instiki.ac.id*; [5]*idabagus.anandita@instiki.ac.id*

ARTICLE INFO

Article history:
Received 17 June 2026
Revised 19 July 2026
Accepted 24 July 2026

Keywords:
tuna eye image;
fish freshness;
PCA;
SVM;
HSV

ABSTRACT

Freshness assessment of tuna (Auxis thazard) in traditional markets still relies mainly on subjective visual inspection, which introduces inconsistency and food-safety risk. This study proposes an objective, low-cost classification pipeline for tuna freshness based on eye images. Six hundred forty fish-eye images were acquired at Kedonganan Fish Market and labeled through a 30-panelist organoleptic test based on SNI 2729:2013. The pipeline segments the eye Region of Interest using U-Net, extracts HSV color features from the segmented eye, reduces dimensionality using Principal Component Analysis (PCA), and classifies freshness with a Support Vector Machine (SVM). A Group K-Fold (k=8) validation scheme and per-fold standardization are used to prevent data leakage across acquisition groups. Grid search over target cumulative variance (50%-95%) and SVM regularization (C=0.1, 1, 10) yields a best configuration at cumulative variance of 55% and C=1, achieving 96.72% accuracy, 97.76% precision, 96.72% recall, and 96.51% F1-score. Compared with SVM without PCA (95.47% accuracy, 215.82 s), the PCA-SVM model reaches equivalent or higher accuracy with 47% lower classification time, supporting deployment on resource-constrained devices.

1. Introduction

Indonesia's status as an archipelagic nation with vast fisheries resources makes reliable post-harvest quality control critical to nutrition and food safety. In traditional markets, freshness assessment of tuna is still dominated by visual inspection, which is prone to subjectivity and inconsistency, while national quality standards such as SNI 2729:2013 require organoleptic evaluation of eyes, gills, and flesh that is difficult to perform reproducibly under market conditions. This gap has direct implications for consumer health, economic loss, and supply-chain inefficiency, and calls for objective, low-cost, non-destructive freshness assessment tools that can be deployed in the field.

Recent studies have demonstrated the effectiveness of image-based fish-freshness assessment. Kilicarslan et al. combined transfer learning (MobileNetV2, Xception, VGG16) with classical machine-learning classifiers to reach very high accuracy on multi-species fish images [1]. Anas et al. used YOLOv5 and Faster R-CNN on hourly-sampled images of tropical marine fish, reporting an F1-score above 98% across three freshness classes [2]. Cho et al. showed that hyperspectral imaging on mackerel eyes and bodies can predict freshness related to TVB-N with accuracy up to 90.14% [3]. For eye-focused pipelines specifically, Adiwidjaja et al. developed a hybrid transfer-learning system on eye and gill color characteristics [4], and Kordkheili et al. demonstrated feature-fusion with SVM classifiers over eye images [5]. In addition, deep-feature approaches based on multi-angle datasets have been shown to generalize across storage conditions [6]. On the Indonesian side, several works focused on tuna: Prasetyo et al. built lightweight CNNs for fish-eye freshness classification [7], and a recent CNN-based system was proposed for classifying tuna loin treatment status in the Indonesian fisheries industry [8].

Within this line of research, the combination of HSV color features with a Support Vector Machine (SVM) classifier has remained a strong baseline because HSV separates hue, saturation, and value channels and is more robust to illumination changes than RGB [9,10]. Syarwani et al. reported 94.28% accuracy for Nile tilapia freshness using HSV and GLCM features fed to an SVM [11]. Rachmat et al. showed that HOG and HSV features together with SVM produce strong species classification across 24 marine-fish classes [12]. Hasym and Susilawati combined PCA with KNN on ornamental fish images, illustrating that dimensionality reduction can preserve discriminative structure while reducing computational cost [13]. Jha et al. combined PCA and SVM to model developmental phases of Ohrid trout, providing further evidence that a PCA-SVM chain simplifies the feature space without degrading accuracy [14].

Despite these advances, most existing eye-based freshness studies for tuna have not simultaneously (i) enforced a leak-safe cross-validation scheme when several images share the same physical fish sample, (ii) quantified the accuracy-vs-latency trade-off introduced by PCA, and (iii) integrated a U-Net segmentation step to isolate the eye Region of Interest (ROI) before feature extraction. Group K-Fold cross-validation has been shown to be essential in avoiding overly optimistic estimates when data are naturally grouped [15,16]. This study addresses this gap by proposing a full pipeline that combines U-Net segmentation, HSV feature extraction, PCA-based dimensionality reduction, and SVM classification, evaluated using Group K-Fold cross-validation. The contribution of this work is threefold: (a) a leak-safe, market-collected tuna eye-image dataset labeled by SNI-based organoleptic evaluation; (b) a systematic grid search characterizing the joint effect of PCA cumulative variance and SVM regularization on classification quality and latency; and (c) empirical evidence that PCA does not necessarily improve raw accuracy but substantially reduces inference time (approximately 47%), which is directly relevant for deployment on low-resource devices in traditional markets.

2. Method

This research is a modeling study on tuna (Auxis thazard) eye images obtained at Kedonganan Fish Market, Badung Regency, Bali, over February-March 2024. Fish were purchased directly from returning boats to guarantee an initial fresh state, and 640 eye images were captured with a 12-megapixel smartphone camera in JPG/PNG (RGB) format together with acquisition metadata. Images were organized into 32 acquisition groups (16 fresh, 16 not-fresh) of 20 images each, so that images sharing the same physical fish sample would remain in the same fold during validation and thus avoid data leakage.

Ground-truth freshness labels were obtained through an organoleptic test based on SNI 2729:2013 [17]. Thirty non-standard panelists scored five physical attributes (eye appearance, gill condition and surface mucus, flesh quality, odor, and texture) on a 1-9 scale. Samples with a mean panel score of 7 or higher were labeled fresh; those below 7 were labeled not fresh.

The processing pipeline is illustrated in Figure 1. It comprises image acquisition, eye Region of Interest (ROI) segmentation using U-Net, preprocessing (resizing to 128x128 pixels and photometric augmentation), HSV feature extraction, group-based data partitioning, per-fold standardization, dimensionality reduction using Principal Component Analysis (PCA), classification using a Support Vector Machine (SVM), and evaluation. Augmentation covered clockwise and counter-clockwise rotation (random 5-45 degrees), horizontal and vertical flips, combined flip-rotation, and shearing on X or Y axes, to simulate the pose and geometric variability expected in field acquisition.

HSV features were extracted from each segmented eye image by aggregating statistics over the H, S, and V channels [9]. PCA was then applied to the standardized feature vectors to retain a chosen fraction of cumulative variance [18,19]. The resulting components were classified using a Support Vector Machine with an RBF kernel [20,21]. Grid search was performed over target cumulative variance (0.50 to 0.95 in steps of 0.05) and SVM regularization parameter C in {0.1, 1, 10}. Group K-Fold cross-validation with k = 8 was used to evaluate each configuration [15]. On every fold, standardization parameters were estimated only on the training partition and then applied to the validation partition, and PCA was refitted per fold, following current data-leakage guidance [16]. Classification quality was measured with accuracy, precision, recall, and F1-score, and computational cost was measured as total PCA fitting time, training time, and evaluation time (seconds) per configuration.

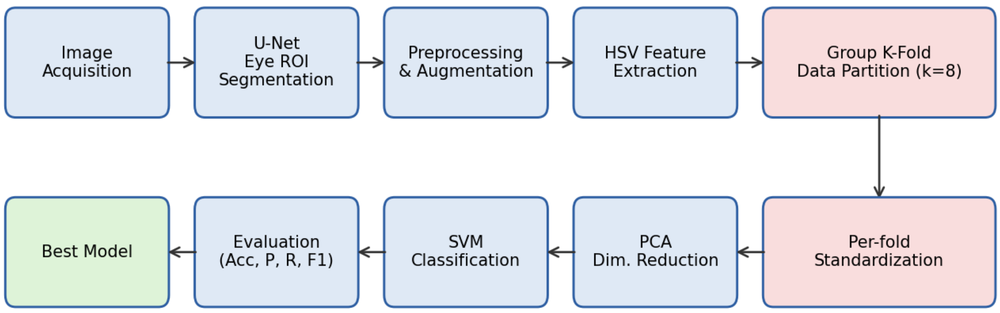

Figure 1. Overall research pipeline for tuna eye-image freshness classification.

[Source: author]

Classification quality is measured using standard confusion-matrix metrics [22]. For a binary problem, given true positives (TP), true negatives (TN), false positives (FP), and false negatives (FN), the metrics used are:

$$\text{Accuracy} = (TP + TN) / (TP + TN + FP + FN) \tag{1}$$

$$\text{Precision} = TP / (TP + FP) \tag{2}$$

$$\text{Recall} = TP / (TP + FN) \tag{3}$$

$$F1 = 2 \times (\text{Precision} \times \text{Recall}) / (\text{Precision} + \text{Recall}) \tag{4}$$

3. Result and Discussions

3.1. Dataset

The dataset consists of 640 tuna eye images acquired at Kedonganan Fish Market, evenly split into 320 fresh and 320 not-fresh samples. All images were captured with a 12-megapixel smartphone camera in JPG or PNG format using the RGB color space. Each sample was linked to metadata identifying its acquisition batch, and images were then organized into 32 acquisition groups of 20 images each (16 fresh groups and 16 not-fresh groups), so that all images sharing the same physical fish sample stayed in the same fold during validation and thereby avoided cross-fold data leakage.

Ground-truth freshness labels were assigned through an organoleptic panel of thirty non-standard panelists following SNI 2729:2013 [17]. Panelists rated five physical attributes on a 1–9 interval scale: eye appearance, gill and mucus condition, flesh quality, odor, and texture. Samples whose mean panel score was 7 or higher were labeled as fresh; the remainder were labeled as not fresh. Figure 2 shows representative eye ROI samples after U-Net segmentation for both classes: fresh eyes are visibly clearer and glossier, while not-fresh eyes show a cloudier lens and reduced saturation, which is the visual cue the HSV feature extractor is expected to capture.

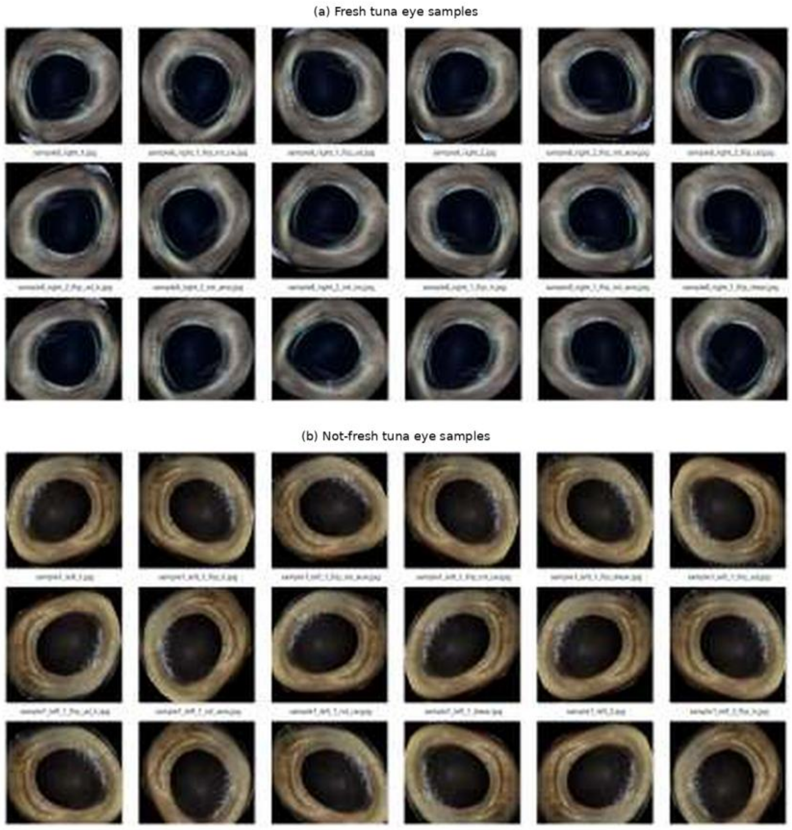

Figure 2. Representative eye ROI samples in the dataset: (a) fresh and (b) not-fresh tuna eyes after U-Net segmentation.

[Source: authors' experimental results]

3.2. Pre-Processing

The pre-processing stage prepares the raw acquired images for feature extraction and classification. It consists of three sub-steps: image resizing, data augmentation, and HSV feature extraction.

First, every segmented eye ROI is resized to a fixed 128 x 128 pixels resolution. This step ensures a consistent input dimension across all samples and reduces computational complexity without discarding the visual cues that distinguish fresh from not-fresh eyes. Second, the training set is expanded through nine geometric augmentation operators applied to each source image: counter-clockwise random rotation (5-45 degrees), clockwise random rotation, horizontal flip combined with counter-clockwise rotation, horizontal flip combined with clockwise rotation, vertical flip, horizontal flip, horizontal followed by vertical flip, X-Y shearing with random shear factor in the range [-0.3, 0.3], and horizontal flip combined with shearing. Reflected borders are used during rotation and shearing to avoid black margins. This augmentation regime simulates the pose, orientation, and mild perspective variability that is expected during in-field acquisition and increases the effective size of the training dataset.

Finally, each augmented image is converted from RGB to the HSV color space, and per-channel statistics on Hue, Saturation, and Value are aggregated into the feature vector used by the classifier. HSV is used rather than RGB because it separates chromatic information (Hue and Saturation) from illumination (Value), which makes the extracted color features more robust to the lighting variations encountered in traditional-market acquisition [9,12]. Figure 3 illustrates the pre-processing steps: (a) the resized eye ROI, (b) representative augmentation variants, and (c) the RGB to HSV conversion applied to both a fresh and a not-fresh sample.

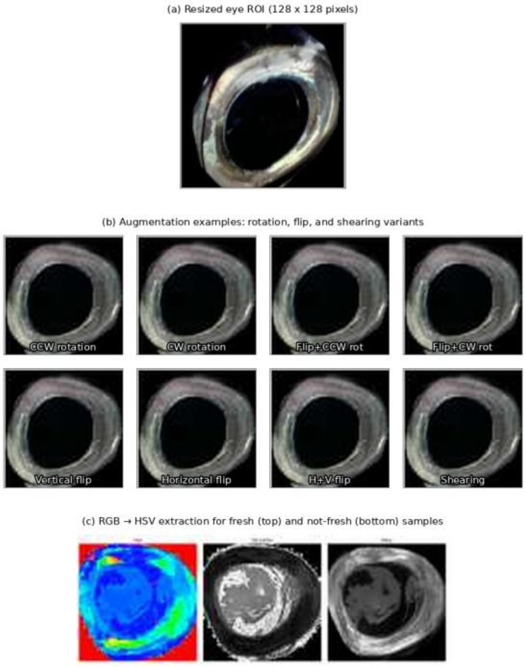

Figure 3. Pre-processing pipeline illustration: (a) resized eye ROI to 128 x 128 pixels, (b) selected augmentation variants (rotation, flip, and shearing), and (c) RGB → HSV extraction for a fresh and a not-fresh sample.

[Source: authors' experimental results]

3.3. Tuna Eye Freshness Detection Results

Before the quantitative grid-search evaluation, the end-to-end pipeline was tested on unseen tuna images to verify that the trained model can output a usable freshness prediction from a single input image. The prediction flow first loads the trained U-Net segmentation model to isolate the eye Region of Interest, then applies the saved PCA-SVM classifier (target cumulative variance 0.55 and C = 1) to output both a class label and a confidence percentage. Figure 4 illustrates this flow on a representative sample.

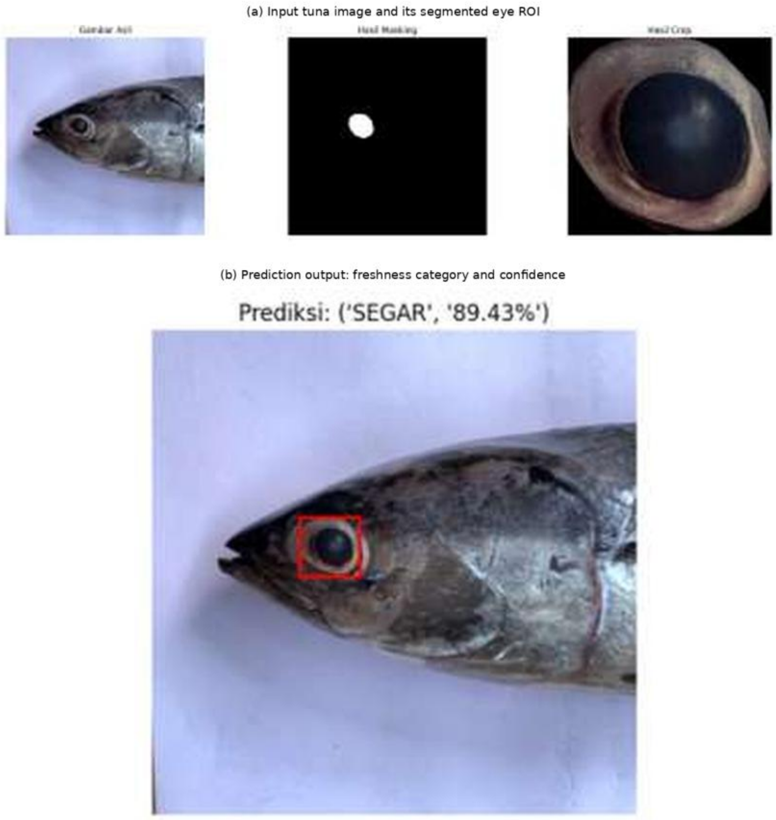

Figure 4. Detection result on a representative input: (a) full tuna image with the segmented eye ROI produced by U-Net, and (b) predicted freshness category together with the model's confidence score.

[Source: authors' experimental results]

Qualitatively, U-Net consistently localized the eye ROI across all tested inputs even when the fish was placed against varied backgrounds, and the PCA-SVM model was able to output a stable freshness score without additional post-processing. This confirms that the pipeline components work together as intended and motivates the systematic quantitative evaluation reported in the remainder of this section.

3.4. Effect of PCA and SVM Regularization

Two experiments were conducted: SVM classification with PCA and SVM classification without PCA. In both experiments, three levels of SVM regularization parameter C were tested (0.1, 1, 10). For the PCA-SVM experiment, PCA target cumulative variance was varied from 0.50 to 0.95 in steps of 0.05.

Table 1. Best PCA-SVM results per regularization value C.

C	Best cum. variance	Test Accuracy	Test Precision	Test Recall	Test F1
0.1	0.50	0.9656	0.9761	0.9656	0.9635
1	0.50 - 0.55	0.9672	0.9776	0.9672	0.9651
10	0.50 - 0.55	0.9672	0.9776	0.9672	0.9651

[Source: authors' experimental results]

The best overall configuration is obtained at target cumulative variance in the 0.50-0.55 range with C = 1, giving test accuracy 96.72%, precision 97.76%, recall 96.72%, and F1-score

96.51%. Setting C = 10 produces identical classification quality but higher training time, indicating that further increasing the regularization parameter beyond C = 1 offers no benefit. Figure 5 shows the joint effect of C and cumulative variance on test accuracy. For C = 0.1 the accuracy decreases monotonically from 96.56% to 93.28% as more variance is retained, while for C in {1, 10} the accuracy remains stable in the 96.2-96.7% range across the tested spectrum.

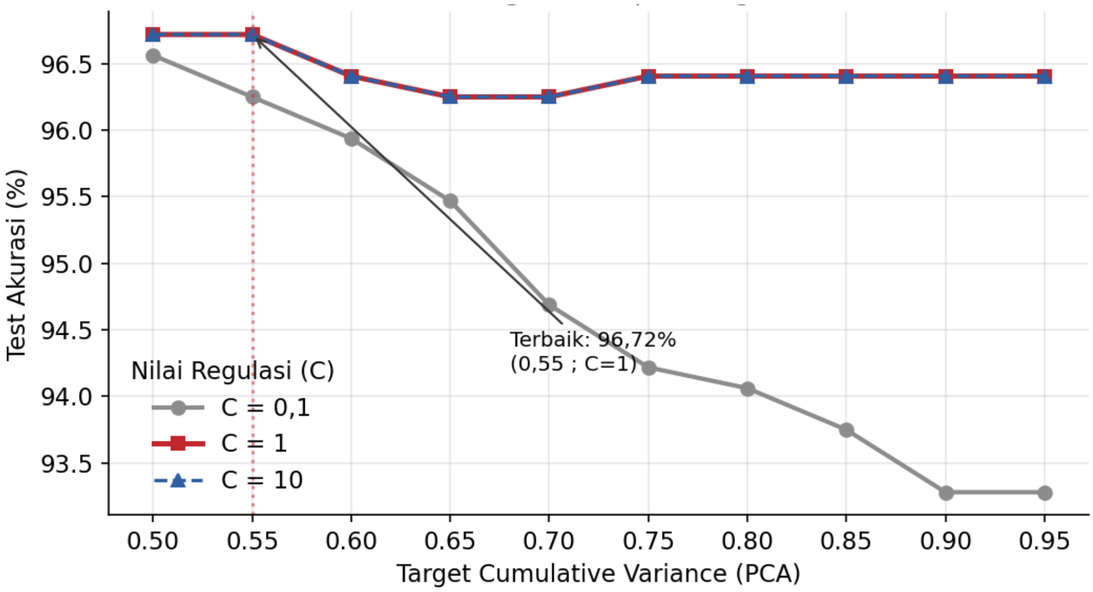

Figure 5. Test accuracy of SVM with PCA versus target cumulative variance for C = 0.1, 1, and 10.

[Source: authors' experimental results]

Table 2. Timing of PCA-SVM classification per target cumulative variance (C = 1).

Cum. Variance	PCA Time (s)	Training (s)	Evaluation (s)	Total (s)
0.50	125.53	0.104	0.208	125.85
0.55	113.34	0.082	0.212	113.63
0.60	117.65	0.122	0.365	118.14
0.65	116.79	0.135	0.325	117.25
0.70	116.80	0.157	0.500	117.46
0.75	118.32	0.201	0.703	119.22
0.80	115.86	0.249	0.715	116.83
0.85	115.53	0.306	0.920	116.76
0.90	116.38	0.653	1.227	118.26
0.95	116.92	0.897	1.701	119.52

[Source: authors' experimental results]

As reported in Table 2, the fastest configuration is obtained at cumulative variance 0.55 (total 113.63 s), not at the lowest tested variance (0.50). This confirms that the reduced-feature representation at 0.55 offers the best balance between compression and discrimination for SVM. Figure 6 visualizes the timing pattern, showing that PCA-SVM stays within a narrow 113-120 s range across the full variance sweep.

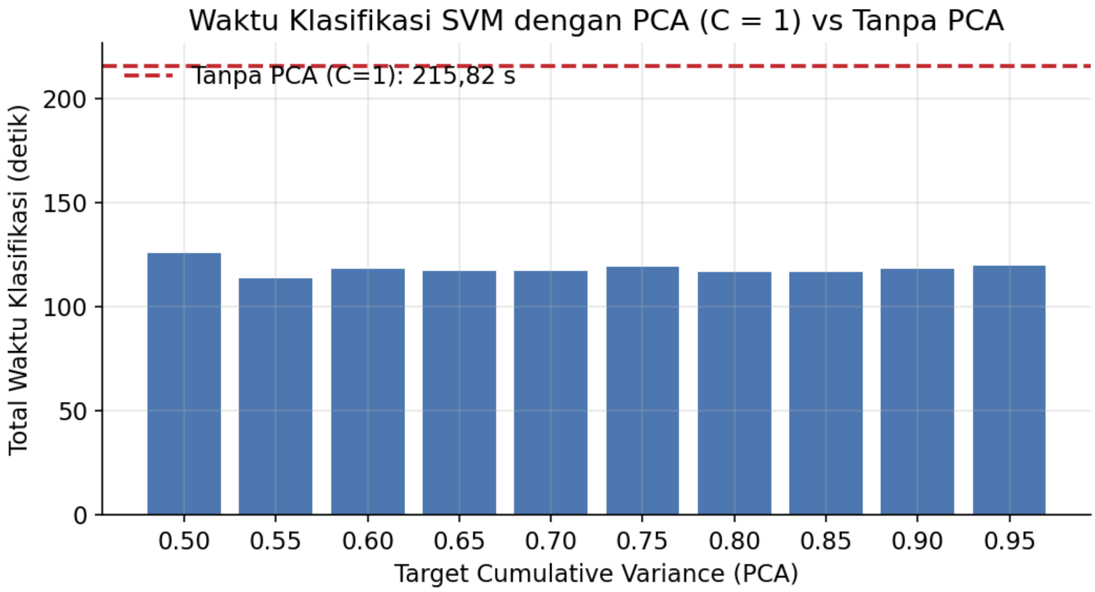

Figure 6. Total classification time of PCA-SVM (C = 1) across target cumulative variance, with SVM-only baseline (dashed line).

[Source: authors' experimental results]

Table 3. Results of SVM classification without PCA.

C	Train Score	Test Accuracy	Test Precision	Test Recall	Test F1
0.1	0.9958	0.9125	0.9370	0.9125	0.9084
1	1.0000	0.9547	0.9674	0.9547	0.9518
10	1.0000	0.9547	0.9674	0.9547	0.9518

[Source: authors' experimental results]

Table 4. Timing of SVM without PCA classification.

C	Training (s)	Evaluation (s)	Total (s)
0.1	90.85	201.45	292.30
1	64.22	151.60	215.82
10	70.35	147.59	217.94

[Source: authors' experimental results]

When PCA is removed, the best SVM configuration still requires 215.82 s (C = 1) or 217.94 s (C = 10), roughly 1.9 times slower than PCA-SVM at the same C. Figure 7 compares accuracy across the four evaluation metrics for the best PCA-SVM and the best non-PCA SVM. The PCA-based model is marginally better on every metric (accuracy 96.72% vs 95.47%; precision 97.76% vs 96.74%; recall 96.72% vs 95.47%; F1 96.51% vs 95.18%), indicating that dimensionality reduction does not degrade classification quality on this dataset.

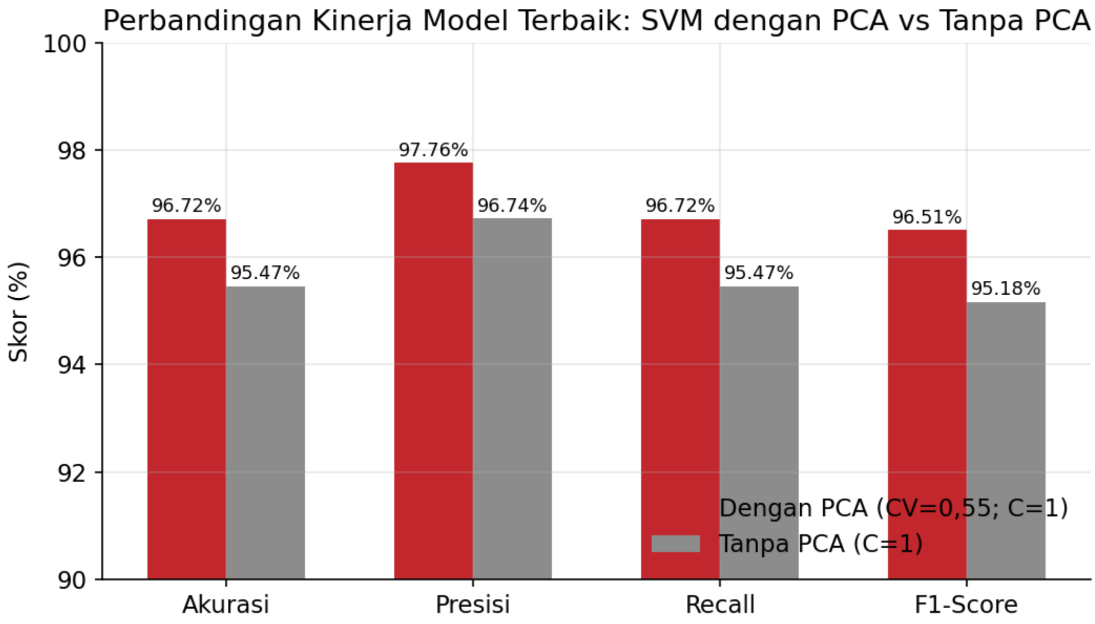

Figure 7. Metric comparison between the best PCA-SVM (cum. var. 0.55, C = 1) and SVM without PCA (C = 1).

[Source: authors' experimental results]

Figure 8 confirms that the largest practical difference between the two settings is on the latency side: the PCA-based configuration is approximately 47% faster than the non-PCA baseline. This is directly relevant for deployment on low-resource devices such as smartphones or single-board computers in traditional markets, where inference latency directly impacts usability.

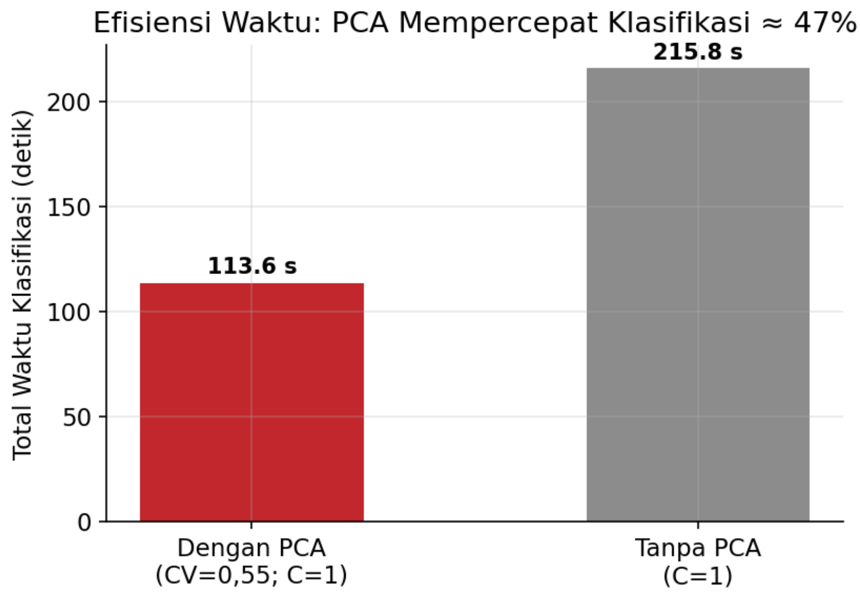

Figure 8. Total classification time: best PCA-SVM vs SVM without PCA (both at C = 1).

[Source: authors' experimental results]

The obtained accuracy is in line with recent HSV-SVM approaches on other fish species. Syarwani et al. reported 94.28% on Nile tilapia [11]; Rachmat et al. reported comparable numbers across 24 marine-fish classes using HOG and HSV with SVM [12]. Compared to Naïve Bayes on tuna eye images which yielded 80% accuracy in a separate study [10], the proposed PCA-SVM pipeline offers substantially higher accuracy on a target-species dataset. Compared with modern deep-learning baselines (MobileNet-based freshness models [7], YOLOv5-based multi-class systems [2], and hyperspectral-based mackerel freshness models [3]), the current approach requires substantially less computational infrastructure while remaining competitive in accuracy on binary freshness. The result also demonstrates that a leak-safe Group K-Fold procedure, together with per-fold standardization, produces stable and reproducible estimates of model performance [15,16], which is particularly important in market-collected datasets where multiple images may share a physical origin.

4. Conclusion

This research designed and evaluated an objective pipeline for tuna freshness classification from eye images, combining U-Net-based ROI segmentation, HSV feature extraction, PCA-based dimensionality reduction, and SVM classification, validated using a Group K-Fold procedure. The best configuration (target cumulative variance 0.55, C = 1) reached 96.72% test accuracy, 97.76% precision, 96.72% recall, and 96.51% F1-score, and reduced total classification time by approximately 47% compared to SVM without PCA. Dimensionality reduction did not degrade classification quality on this dataset, and Group K-Fold validation avoided the leakage that would have otherwise inflated the estimated performance. Future work should extend the dataset to more acquisition sites, seasons, and species; explore multi-class freshness levels beyond binary; incorporate texture features such as GLCM alongside HSV; test lightweight deep architectures under the same leak-safe protocol; and package the model into a mobile application to make the tool practically available to traders and consumers in traditional markets.

Acknowledgment

This research is funded by the Directorate of Research, Community Service, and Innovation of the Institut Bisnis dan Teknologi Indonesia through the INSTIKI Research and Development Program (IRDP). The authors thank the fishers and traders at Kedonganan Fish Market for supporting sample acquisition, and the panelists who conducted the organoleptic evaluation.

References

[1] S. Kılıçarslan, M. M. Hız Çiçekliyurt, and S. Kılıçarslan, "Fish freshness detection through artificial intelligence approaches: a comprehensive study," Turkish J. Agric. - Food Sci. Technol., vol. 12, no. 2, pp. 290-295, 2024, doi: 10.24925/turjaf.v12i2.290-295.6670.

[2] D. F. Anas, I. Jaya, and Y. Herdiyeni, "Measurement and analysis of detecting fish freshness levels using deep learning method," IJCCS (Indones. J. Comput. Cybern. Syst.), vol. 18, no. 4, 2024, doi: 10.22146/ijccs.95054.

[3] J.-S. Cho et al., "Determination of freshness of mackerel (Scomber japonicus) using shortwave infrared hyperspectral imaging," Foods, vol. 12, no. 12, p. 2305, 2023, doi: 10.3390/foods12122305.
[4] A. Ismail et al., "A novel hybrid system for automatic detection of fish quality from eye and gill color characteristics using transfer learning technique," PLOS ONE, vol. 18, no. 4, e0284804, 2023, doi: 10.1371/journal.pone.0284804.
[5] O. Zare Kordkheili et al., "Fish freshness detection from eye images using feature-based fusion and Support Vector Machine classifier," Iranian J. Fisheries Sci., 2024, doi: 10.22092/ijfs.2024.363504.
[6] Y. Kılıç et al., "Deep learning-based prediction of fish freshness and purchasability using multi-angle image data," Foods, vol. 15, no. 1, p. 68, 2026, doi: 10.3390/foods15010068.
[7] E. Prasetyo, R. Purbaningtyas, R. D. Adityo, N. Suciati, and C. Fatichah, "Combining MobileNetV1 and depthwise separable convolution bottleneck with expansion for classifying the freshness of fish eyes," Inf. Process. Agric., vol. 9, no. 4, pp. 485-496, 2022, doi: 10.1016/j.inpa.2022.01.002.
[8] F. R. Muhaidat, A. J. Latumakulita, and R. R. Ramadhan, "A deep learning approach to automated treatment classification in tuna processing: enhancing quality control in Indonesian fisheries," Fishes, vol. 10, no. 2, p. 75, 2025, doi: 10.3390/fishes10020075.
[9] A. Sukarni, A. Qashlim, and I. Djufri, "Sistem pengolahan citra untuk mengidentifikasi kesegaran ikan menggunakan citra digital mata," J. Peqguruang: Conf. Ser., vol. 5, no. 1, 2023, doi: 10.35329/jp.v5i1.3694.
[10] N. Rachmat, Y. Yohannes, and J. Iskandar, "Klasifikasi jenis ikan laut menggunakan metode SVM dengan fitur HOG dan HSV," JATISI (Jurnal Teknik Informatika dan Sistem Informasi), vol. 8, no. 4, 2021, doi: 10.35957/jatisi.v8i4.1686.
[11] M. I. Syarwani, G. S. Nugraha, F. Mardhotillah, and F. Bimantoro, "Classification of Nile tilapia's freshness based on eyes and gills using Support Vector Machine," in Proc. First Mandalika Int. Multi-Conf. Sci. Eng. (MIMSE 2022), 2022, doi: 10.2991/978-94-6463-084-8_15.
[12] A. Alkaraz, H. Fadhel, and M. Al-Radhi, "Accurate segmentation of vegetation in UAV desert imagery using HSV-GLCM features and SVM classification," J. Imaging, vol. 12, no. 1, p. 9, 2026, doi: 10.3390/jimaging12010009.
[13] I. E. Hasym and I. Susilawati, "Klasifikasi jenis ikan cupang menggunakan algoritma Principal Component Analysis (PCA) dan K-Nearest Neighbors (KNN)," KONSTELASI: Konvergensi Teknologi dan Sistem Informasi, vol. 1, no. 1, 2021, doi: 10.24002/konstelasi.v1i1.4242.
[14] S. K. Jha, I. Uzunov, et al., "A combined approach of Principal Component Analysis and Support Vector Machine for early development phase modeling of Ohrid trout (Salmo letnica)," CMES - Comput. Model. Eng. Sci., vol. 126, no. 3, 2021, doi: 10.32604/cmes.2021.011821.
[15] S. Bates, T. Hastie, and R. Tibshirani, "Cross-validation: what does it estimate and how well does it do it?," J. Am. Stat. Assoc., vol. 119, no. 546, pp. 1434-1445, 2024, doi: 10.1080/01621459.2023.2197686.
[16] R. R. C. Palma-Fraga et al., "When k-fold cross-validation gets biased: analysis under time-series and grouped data," Proc. Hum. Factors Ergon. Soc. Annu. Meet., vol. 67, no. 1, pp. 2162-2167, 2023, doi: 10.1177/21695067231192258.
[17] Badan Standardisasi Nasional, "SNI 2729:2013 Ikan Segar," Badan Standardisasi Nasional Indonesia, 2013.
[18] M. J. Y. Mutinda and G. K. Langat, "Exploring the role of dimensionality reduction in enhancing machine learning algorithm performance," Asian J. Res. Comput. Sci., vol. 17, no. 5, 2024, doi: 10.9734/ajrcos/2024/v17i5445.

[19] Y. Zhang and J. Su, "Data dimensionality reduction using Principal Component Analysis: a case study," in Proc. IEEE Int. Conf. Comput. Sci. Elec. Eng. (ICCSEE), 2024, doi: 10.1109/ICCSEE55467.2024.10593421.

[20] Y. Xu, X. Zhou, and C. Zhang, "Exploring kernel machines and Support Vector Machines: principles, techniques, and future directions," Mathematics, vol. 12, no. 24, p. 3935, 2024, doi: 10.3390/math12243935.

[21] N. Amaya-Tejera, M. Gamarra, J. I. Vélez, and E. Zurek, "A distance-based kernel for classification via Support Vector Machines," Front. Artif. Intell., vol. 7, 1287875, 2024, doi: 10.3389/frai.2024.1287875.

[22] N. Kühl, M. Schemmer, M. Goutier, and G. Satzger, "Artificial intelligence and machine learning," Electronic Markets, vol. 32, no. 4, 2022, doi: 10.1007/s12525-022-00598-0.

[23] L. Vanneschi and S. Silva, "Support Vector Machines," in Natural Computing Series, Springer, 2023, pp. 271-281, doi: 10.1007/978-3-031-17922-8_10.

[24] Z. Su, W. Li, Z. Ma, and R. Gao, "An improved U-Net method for the semantic segmentation of remote sensing images," Applied Intelligence, vol. 52, no. 3, pp. 3276-3288, 2022, doi: 10.1007/s10489-021-02542-9.